J Nanopart Res (2017) 19: 198
DOI 10.1007/s11051-017-3877-8

RESEARCH PAPER

Nanostructured TiO_2 and ZnO prepared by using pressurized hot water and their eco-toxicological evaluation

Ivana Troppová · Lenka Matějová · Hana Sezimová · Zdeněk Matěj · Pavlína Peikertová · Jaroslav Lang

Received: 22 December 2016 / Accepted: 2 May 2017 / Published online: 3 June 2017

Abstract The eco-toxicological effects of unconventionally prepared nanostructured TiO_2 and ZnO were evaluated in this study, since both oxides are keenly investigated semiconductor photocatalysts in the last three decades. Unconventional processing by pressurized hot water was applied in order to crystallize oxide materials as an alternative to standard calcination. Acute biological toxicity of the synthesized oxides was evaluated using germination of *Sinapis alba* seed (ISO 11269-1) and growth of *Lemna minor* fronds (ISO 20079) and was compared to commercially available TiO_2 Degussa P25. Toxicity results revealed that synthesized ZnO as well as TiO_2 is toxic contrary to commercial TiO_2 Degussa P25 which showled stimulation effect to *L. minor* and no toxicity to *S. alba*. ZnO was significantly more toxic than TiO_2. The effect of crystallite size was considered, and it was revealed that small crystallite size and large surface area are not the toxicity-determining factors. Factors such as the rate of nanosized crystallites aggregation and concentration, shape and surface properties of TiO_2 nanoparticles affect TiO_2 toxicity to both plant species. Seriously, the dissolution of Ti^{4+} ions from TiO_2 was also observed which may contribute to its toxicity. In case of ZnO, the dissolution of Zn^{2+} ions stays the main cause of its toxicity.

Keywords Titanium dioxide · Zinc oxide · Pressurized hot water crystallization · Acute biological toxicity · *Lemna minor* · *Sinapis alba* · Nanoparticle · Environmental and health effects

I. Troppová (✉) · L. Matějová · P. Peikertová · J. Lang
Institute of Environmental Technology, VŠB-Technical University of Ostrava, 17. Listopadu 15/2172, 708 33 Ostrava, Czech Republic
e-mail: ivana.troppova@vsb.cz

H. Sezimová
Department of Biology and Ecology, Faculty of Science, University of Ostrava, Chittussiho 10, 710 00 Ostrava, Czech Republic

Z. Matěj
Department of Condensed Matter Physics, Faculty of Mathematics and Physics, Charles University in Prague, Ke Karlovu 5, 121 16 Prague 2, Czech Republic

Introduction

Titanium dioxide (TiO_2) and zinc oxide (ZnO) nanoparticles have general importance as absorbers of ultraviolet (UV) light and broad scale use as pigments in plastics, paints, paper coatings and sunscreen lotions. Both materials are keenly investigated photocatalysts and have been considerably studied for the removal of organic compounds from contaminated air and water and for microbial disinfection (Adams et al. 2006; Coronado et al. 2013; Hoffmann et al. 1995).

The technology and research progress gave rise to manufactured nanomaterials (Laborda et al. 2016). The environmental level of manufactured nanomaterials is expected to increase continually which is given by their current widespread application. It was reported that they may enter natural ecosystems through direct application, biosolid application, accidental release, contaminated

soil/sediments or atmospheric fallout (Rico et al. 2011). However, properties of manufactured nanomaterials differ from their bulk counterparts. Materials that are safe in a bulk form can become harmful in nanoscale. It is well known that the type of preparation and used precursors for synthesis can affect the micro(structural) and surface properties of manufactured nanomaterials significantly (Matějová et al. 2017). Toxicity of nanomaterials was addressed by many authors (Hofmann-Amtenbrink et al. 2015; Hougaard et al. 2015; Wang et al. 2016), but the unified methodology and procedures of toxicity measurement do not exist yet. First steps in this field have been done recently (Arts et al. 2015; Rasmussen et al. 2016).

Concerning eco-toxicological effects of ZnO nanoparticles, they have been very limited across all taxa (Kahru and Dubourguier 2010). The studies have identified toxic effects of ZnO nanoparticles in both aquatic and terrestrial species; toxicity can occur at concentration around 1 mg/l. This suggests that ZnO nanoparticles, when reaching a certain level in natural environments, can cause significant risk to the environmental biota (Ma et al. 2013). ZnO nanoparticles cause phytotoxicity in a limited number of crops such as *Raphanus sativus*, *Brassica napus*, *Lactuca sativa*, *Zea mays* and *Cucumis sativus* (Lin and Xing 2007), *Allium cepa* (Kumari et al. 2011) and *Vicia faba* (Manzo et al. 2011). High doses of ZnO nanoparticles have negative impacts on agricultural ecosystem such as declines in soil quality (Priester et al. 2012), reduces growth and biomass (Yoon et al. 2014) and excessive Zn accumulation in plant tissues and seeds (Mukherjee et al. 2014; Priester et al. 2012). However, there are still several knowledge gaps which need to be filled to gain a thorough understanding on ZnO nanoparticles eco-toxicity for risk assessment and management. First, there is a significant lack of characterizations for ZnO nanoparticles and the exposure system in eco-toxicity studies conducted thus far. Since ZnO nanoparticles can elicit toxicity by different modes of action (i.e. particle dissolution, photo-activation etc.) and these modes of action are highly dependent on exposure conditions such as water chemistry of exposure media, irradiation conditions, a thorough characterization of these exposure conditions is essential for proper interpretation of toxicity data as well as valid comparison between different studies. Second, tools and techniques are needed in order to differentiate between the particle-induced toxicity and dissolved Zn^{2+} ions effects. Third, there are no sufficient data on chronic effects from long-term and low-concentration exposure, which may be more representative for real environmental exposure (Ma et al. 2013).

Concerning eco-toxicological effects of TiO_2 nanoparticles, the fate and the long-term effects of this nanomaterial remain unrevealed as well as its impact and risk assessment are also challenging. TiO_2 nanoparticles can interact with both biotic and abiotic components of the environment. These interactions rely mostly on their agglomeration or aggregation state. This determines the size in which they are present in the environment and consequently their potential for transport and sedimentation and for uptake by organisms (Adam et al. 2015). It was reported that TiO_2 nanoparticles cause toxicity to organisms by producing reactive oxygen species upon interaction with UV light, leading to cell membrane damage (Manke et al. 2013; Sadiq et al. 2011). Jacob et al. (2013) observed that TiO_2 nanoparticles play a key role in the modification of activities of enzymatic antioxidants at concentration of 10 and 30 ppm. Moreover, in spinach seedlings, 0.25% of TiO_2 nanoparticles resulted in the generation of oxidative stress in chloroplasts, and TiO_2 nanoparticles caused elimination of microtubules in *Arabidopsis thaliana* (Tripathi et al. 2017).

As it was indicated above, the problem of manufactured nanomaterials' toxicity is even more complex, since the tests being done on pristine nanoparticles under controlled laboratory conditions do not account for their interaction with the real environment. As Bour et al. (Bour et al. 2015) and Judy et al. (Judy and Bertsch 2014) suggest, the studies of nanomaterial toxicity should be carried out in more realistic conditions, and as Menard et al. (Menard et al. 2011) stresses out, the manufactured nanomaterials' physicochemical properties should be thoroughly characterized and known.

According to Sun et al. (Sun et al. 2014), one of the real release pathways for manufactured nanomaterials to the environment is their collection within wastewater and their concentration in waste sludge. Waste sludge is then deposited on landfill or used as a fertilizer on agricultural land. The testing subjects therefore have to encompass the whole cycle of the manufactured nanomaterials in the environment and range from microorganisms like bacteria (Barnes et al. 2013; Bellanger et al. 2015; Farkas et al. 2015; Mallevre et al. 2014) and algae (Fu et al. 2015; Schiavo et al. 2016) to cells (Hsiao and Huang 2011), plants

(Andersen et al. 2016; Clement et al. 2013; Cox et al. 2016), but also fish (Xiong et al. 2011) or mice (Warheit et al. 2015) and others.

This work focuses on the preparation of nanostructured TiO_2 and ZnO by unconventional preparation method using pressurized hot (subcritical) water and evaluation of their acute biological toxicity using germination of *Sinapis alba* seed (ISO 11269-1, 1993) and growth of *L. minor* fronds (ISO 20079, 2005). Since for the preparation of both nanomaterials pressurized hot water crystallization was used, the effect of this post-treatment step on nanomaterial toxicity can be excluded, as water is a non-toxic solvent. The advantage of performed acute biological toxicity tests compared to often used acute aquatic toxicity tests according to the OECD 201 methodology using freshwater green algae (*Desmodesmus subspicatus*, *Chlorella vulgaris*) is the fact that in the tests with *S. alba* seed, the nanoparticulated samples do not have to be dissolved in water, thus, the sedimentation of nanoparticulated samples, which can affect the toxicity results, is eliminated. The indicator organism (*S. alba* seed) and the nanoparticulated sample are left in contact on the filter paper, without the possibility of sedimentation. In tests with *L. minor* fronds, the concentration series of nanoparticles in suspensions are prepared, but the sedimentation is removed by continuous mixing throughout the exposure. Thus, two various experimental arrangements were used for the determination of toxicity of nanoparticulated samples in our study. In both tests with *D. subspicatus* and *C. vulgaris*, the nanoparticulated samples form suspensions after mixing with water and settle down, which can affect the toxicity results. Another fact is the evaluation method. In our tests on *S. alba* and *L. minor*, the determination of growth inhibition is feasible, excluding the turbidity of the tested nanoparticulated samples. In the tests, e.g. on *D. subspicatus*, the results are determined by counting the algal cultures under the microscope, using an automatic cell counting, and this process is influenced highly by the turbidity of the sample.

Experimental

Chemicals

All aqueous solutions for chemical experiments were prepared using deionized water (electrical conductivity ~0.06–0.08 μS/cm). The reference commercial TiO_2 anatase-rutile mixture (TiO_2 Degussa P25) for ecotoxicity studies was obtained from Degussa (Germany). Chemical for preparation of nanostructured materials such as titanyl sulphate ($TiOSO_4$) was purchased from Precheza a.s. (Czech Republic). Sulphuric acid (H_2SO_4, p.a.), sodium hydroxide (NaOH, p.a.), sodium carbonate (Na_2CO_3, p.a.) and zinc chloride ($ZnCl_2$, p.a.) were purchased from Penta a.s. (Czech Republic).

Preparation of precursors for TiO_2 and ZnO nanoparticles preparation

The $TiO(OH)_2$ precursor was prepared via thermal hydrolysis. The stock solution of titanyl sulphate (1.25 mol/dm^3) was diluted to 0.2 mol/dm^3 solution by addition of 0.1 mol/dm^3 sulphuric acid. The 0.2 mol/dm^3 solution of titanyl sulphate was heated, the spontaneous precipitation of $TiO(OH)_2$ occurred at 80 °C. The temperature of 80 °C was kept for 1 h. The pH was adjusted with 5 mol/dm^3 NaOH at pH = 7. After that, the created suspension was left to cool down to ambient temperature. The suspension was filtered, and the filter cake/precipitate was washed to remove the sulphate anions with 4–5 l of deionized water. The precipitate was then dried in Petri dishes at 40 °C overnight. The obtained precipitate was subsequently processed by pressurized hot water to prepare nanoparticulated TiO_2.

The $Zn(OH)_2$ precursor was prepared by neutralization. Na_2CO_3 was dissolved in water and mixed on an electromagnetic stirrer until the solution was clear. $ZnCl_2$ was added to the Na_2CO_3 solution and white $Zn(OH)_2$ precipitate started to appear. The Na_2CO_3 was in 50% surplus to $ZnCl_2$. The addition of $ZnCl_2$ was gradual because of CO_2 production. The mixture was stirred for 3 h, filtered and washed with deionized water until the pH was 7. The precipitate was dried overnight at 50 °C and powdered in a mortar. The obtained precipitate was subsequently processed by pressurized hot water to prepare nanoparticulated ZnO.

Both precursors were sieved for high-pressure processing to particle-size fraction of 0.160–0.315 mm.

Processing of precursors by pressurized hot (subcritical) water

Deionized water (electrical conductivity ~0.06–0.08 μS/cm) was used as a solvent for pressurized hot water processing. Processing by pressurized hot water was

carried out in a laboratory-made unit equipped with a HPLC BETA10 Plus gradient pump (Ecom s.r.o., Czech Republic), a chromatographic oven operating in the temperature range of 25–400 °C, a capillary cooling and a restrictor operating at ambient temperature. A scheme of the experimental setup is shown in Fig. 1a. The TiO_2 precursor was placed in a 24-ml high-temperature stainless-steel cell and was processed in a flow regime at pressure of 10 MPa and temperature of 100 °C using 1.05 l of deionized water. The ZnO precursor was placed in a 10-ml high-temperature stainless-steel cell and was processed in a flow regime at pressure of 30 MPa and temperature of 250 °C using 1.5 l of deionized water. The flow rate of water during the high-pressure processing was kept at 3.5–4.5 ml/min. Since both precursors were powders, their special arrangement in the high-temperature stainless-steel cell was used (Fig. 1b) to prevent the plugging of frits inside the cell. The different experimental conditions of processing for both precursors by pressurized hot water were selected based on previous photocatalytic investigations in AO7 photodegradation, when both oxides at selected processing conditions were the most photoactive.

Acute biological toxicity tests

The acute biological toxicity of prepared nanomaterials (TiO_2, ZnO, TiO_2 Degussa P25) was determined using the *L. minor* plant growth test and the *S. alba* seed germination test. For toxicity tests, the nanoparticulated materials were crashed and sieved to particle-size fraction of <0.160 mm.

The *L. minor* plant test (ISO 20079, 2005) measured the growth inhibition of fronds in the presence of nanoparticulated material compared to the control samples containing only the culture medium. The tests were performed in the growth chamber with the light luminosity of 10,000 lx. *L. minor* fronds grow as monocultures in different concentrations of the tested substance over a period of 7 days. The objective of the test is to quantify the substance-related effects on vegetative growth over this period based on assessments of frond number and also on assessments of biomass. To quantify the substance-related effects, the growth in the tested solutions is compared with that of the controls and the concentration bringing the specified 50% inhibition of growth is determined and expressed as the EC_{50} value (Quality 2005).

In the seed germination test, the *S. alba* (ISO 11269-1, 1993) was used. Inhibition of root growth after 3 days exposure was measured. The tests with *S. alba* were performed in the darkness in the tempered bath at constant temperature of 21 °C. The test was considered to be valid if the germination of the control sample was ≥90%, and the standard deviation (SD) value was inferior to the double SD value measured in the control (containing only the culture medium). The inhibition concentration value IC_{50} was derived after plotting the percentage of inhibition of root growth against the concentration.

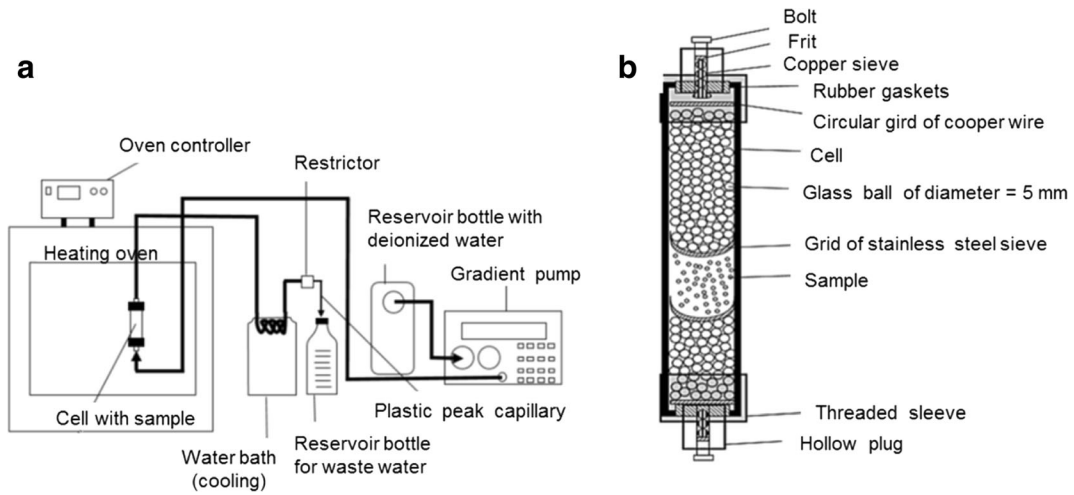

Fig. 1 Illustration of **a** set-up for pressurized hot water processing and **b** high-temperature stainless-steel cell with arrangement of precursor

The nanoparticulated materials were tested in a concentration range 0.01–10 mg/ml for *L. minor* and 1–180 mg/ml for *S. alba*.

The positive controls using toxicants recommended in the corresponding ISO standard: 3.5-dichlorophenol and potassium dichromate were also measured to check the sensitivity of the individual tests. The acute biological toxicity tests were performed three times in parallel repetitions.

Characterization of investigated nanoparticulated materials

Nitrogen physisorption at 77 K was performed on a 3Flex automated volumetric apparatus (Micromeritics Instruments, USA) after degassing of materials at 150 °C for more than 18 h under vacuum below 1 Torr. Degassing at low temperature was applied to remove physisorbed water but having no influence on the porous morphology of the developed materials. The specific surface area, S_{BET}, was calculated according to the classical Brunauer–Emmett–Teller (BET) theory for the *p/p0* range of 0.05–0.30 (Gregg and Sing 1982). As the specific surface area, S_{BET}, is not a proper parameter in the case of mesoporous solids containing micropores (Schneider 1995), the mesopore surface area, S_{meso}, and the micropore volume, V_{micro}, were also evaluated based on the t-plot method (de Boer et al. 1966) with the C_{modif} constant (Lecloux and Pirard 1979; Schneider 1995). The net pore volume, V_{net}, was determined from the nitrogen adsorption isotherm at maximum *p/p0* (~0.99). The pore-size distribution was evaluated from the adsorption branch of the nitrogen adsorption-desorption isotherm by the Barrett–Joyner–Halenda (BJH) method (Barrett et al. 1951) using the de Boer standard isotherm and assuming cylindrical pore geometry.

X-ray diffraction (XRD) patterns were recorded using a Bruker D8 Advance diffractometer (Bruker AXS) equipped with a fast position-sensitive detector VÅNTEC 1. CoKα irradiation (λ = 0.178897 nm) was used. Measurements of all samples were carried out in reflection mode in symmetrical Bragg–Brentano arrangement.

Fourier-transform infrared (FTIR) spectra were recorded in the range of 400–4000/cm. Samples were measured by ATR technique with diamond crystal on Nicolet 6700 FTIR (Thermo Scientific, USA).

Raman spectra were collected on a XploRA™ Smart System composed of microscope and Raman spectrometer (Horiba Jobin Yvon, France) using 532 nm laser source. The Olympus microscope BX 41/51 with an objective magnification of 50 was used to focus the laser beam on the sample placed on an X–Y motorized sample stage. The filter to reduce laser beam to 25% of initial laser beam and grating 1200 grooves/mm were used.

Scanning electron microscopy with chemical analysis (SEM-EDX) was performed using a Philips XL30 scanning electron microscope (SEM) with energy dispersive X-ray microanalysis (EDX). The SEM images were obtained using back-scattered electrons at an operating voltage of 25 kV.

Transmission electron microscopy (TEM) analysis was done on a JEOL 2100 at 200 kV of accelerating voltage. Prior to analysis, purified and ultra-sonified water for 3 min was added to powder sample placed in small Eppendorf tube. Suspensions were dropped on a copper grid with holey carbon film and dried on air.

The samples of aqueous growing media from *L. minor* tests containing specified weight to volume ratios of ZnO and TiO_2 were measured on a ContrAA 700 atomic absorption spectrometer (AAS) (Analytik Jena, Germany) by electrothermal atomization technique in with L'vov platform tube.

Results and discussion

Characterization of prepared nanoparticulated materials

Evaluated textural and (micro)structural properties of both prepared materials from nitrogen physisorption and XRD measurements, respectively, are summarized in Table 1 (Matejova et al. 2013) and Fig. 2a, b. While prepared TiO_2 shows mesoporous structure with 165 m^2/g mesopore surface area and minor contribution of micropores, ZnO shows mesoporous-macroporous structure possessing low surface area of 17 m^2/g. The structural properties correspond well with evaluated textural properties; TiO_2 of anatase crystal structure is nanocystalline with ~7 nm anatase crystallites (Fig. 2a), while ZnO of wurtzite crystal structure possesses ~114 nm crystallites. Moreover, beside ZnO wurtzite also Zn_2SiO_4 willemite of ~88 nm crystallite size was clearly identified in prepared ZnO (Table 1, Fig. 2b). The presence of Zn_2SiO_4 willemite (RRUFF 2016) can

Table 1 Textural and structural properties of investigated nanoparticulated materials

Material	Nitrogen physisorption				XRD	
	S_{BET} (m^2/g)	S_{meso} (m^2/g)	V_{micro} (mm^3_{liq}/g)	V_{net} (mm^3_{liq}/g)	Phase composition (wt.%)	Volume-weighted crystallite size (nm)
TiO_2	240	165	50	223	100 wt.% anatase	6.9
ZnO	17	15	2.6	130	71 wt.% wurtzite (ZnO)	114
					29 wt.% willemite (Zn_2SiO_4)	88
TiO_2 Degussa P25 (Matejova et al. 2013)	50	31	10	211	80 wt.% anatase 20 wt.% rutile	~25[a] ~54

[a] The average primary crystallite size stated by producer

be explained by preparation procedure; during high-pressure processing using pressurized hot water, Zn^{2+} ions were released to hot water from the $Zn(OH)_2$ precursor and these Zn^{2+} ions reacted with SiO_2 present in the glass balls which were used as filling substrate in the extraction cell (glass balls were mainly composed of SiO_2, Na_2O and CaO).

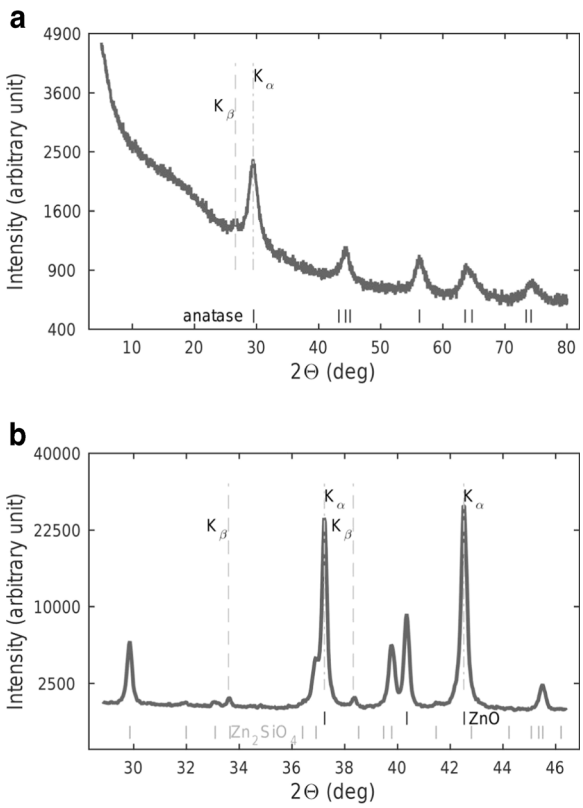

Fig. 2 XRD pattern of prepared **a** TiO_2 and **b** ZnO. Note: In spectra, there are visible Co K-beta line artefacts from X-ray tube

Measured FTIR spectra of TiO_2 precursor and nanoparticulated TiO_2 are shown in Fig. 3. From the spectra (Fig. 3), it is evident that there are no significant differences between these materials. The most intensive bands at 3201 cm^{-1} and 1629 cm^{-1} correspond to the O-H stretching and deformation vibrations, respectively. Broad band under 1000 cm^{-1} has similar progress as ordinary TiO_2 anatase spectrum. The Raman spectra in Fig. 4 prove the similarity of TiO_2 precursor and nanoparticulated TiO_2. Both spectra show all characteristic bands of anatase modification of TiO_2. All these facts indicate that in case of preparation of nanoparticulated TiO_2 by thermal hydrolysis using titanyl sulphate, the TiO_2 anatase crystallization occurs already during the thermal hydrolysis preparation of the precursor.

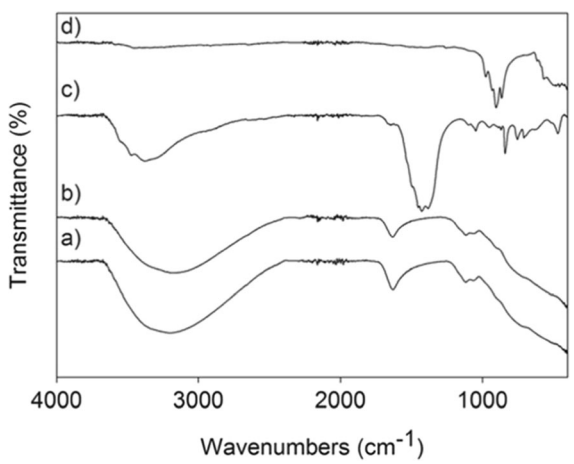

Fig. 3 FTIR spectra of TiO_2 precursor (*a*), nanoparticulated TiO_2 (*b*), ZnO precursor (*c*) and ZnO (*d*)

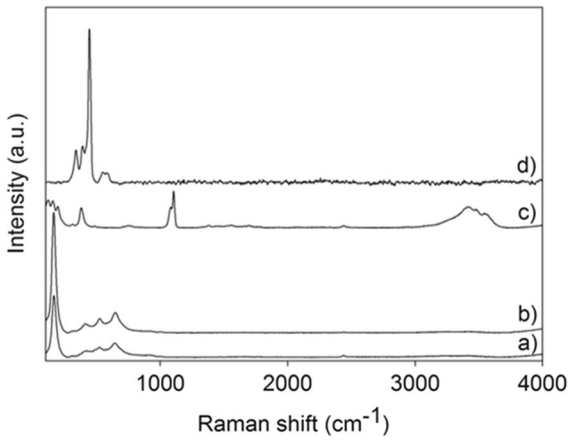

Fig. 4 Raman spectra of TiO_2 precursor (*a*), nanoparticulated TiO_2 (*b*), ZnO precursor (*c*) and ZnO (*d*)

In Fig. 3, the FTIR spectra of ZnO precursor and nanoparticulated ZnO are shown as well. A broad and intensive band at 3374 cm^{-1} and shoulder at 1648 cm^{-1} belong to the O-H vibrations. According to all presented bands in the spectrum of ZnO precursor (Fig. 3c), it can be estimated that the ZnO precursor is composed of hydrozincite ($Zn_5(OH)_6(CO_3)_2$), which being often used precursor. FTIR spectrum of ZnO (Fig. 3d) shows two characteristic bands at 420 and 486 cm^{-1} which are not clearly visible in the spectrum. On the other hand, a strong structured band around 900 cm^{-1} is presented in the spectrum and corresponds to the willemite (Zn_2SiO_4), which presence was proved also by XRD. Similar conclusions were obtained from Raman measurements (Fig. 4), where the most intensive band at 1080 cm^{-1} of ZnO precursor belongs to the presence of carbonate (Fig. 4c). The Raman spectrum of ZnO (Fig. 4d) corresponds to the typical ZnO spectrum. No bands corresponding to Zn_2SiO_4 willemite were observed, but this feature may be caused by strong Raman signal of ZnO as well as by used 532 nm laser.

The surface composition and morphology of prepared TiO_2 and ZnO clusters were studied using SEM-EDX technique. EDX spectra of both materials are shown in Fig. 5a, b and reveal that TiO_2 nanoparticles contain only Ti and O elements, contrary to ZnO

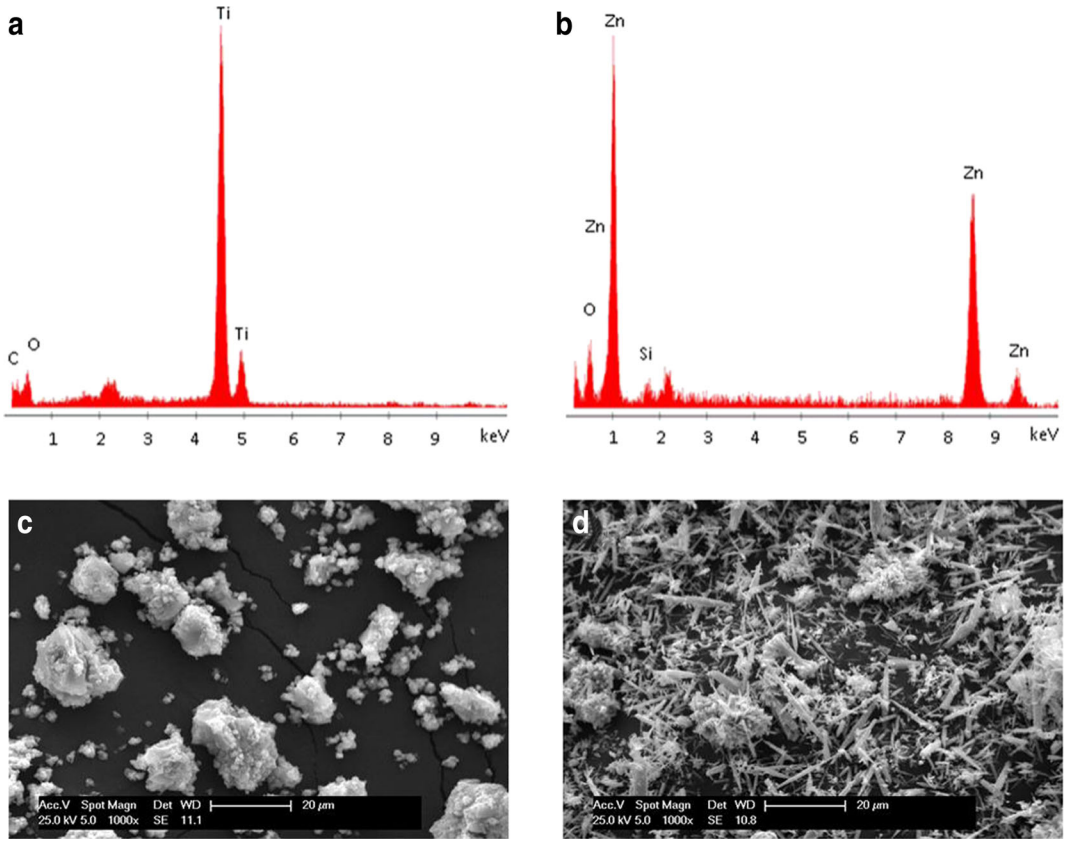

Fig. 5 EDX analysis of investigated **a** TiO_2 and **b** ZnO, and SEM micrographs of investigated **c** TiO_2 and **d** ZnO

nanoparticles which contain besides Zn and O element also Si element. Results from EDX analysis prove the XRD results, where Zn_2SiO_4 willemite was identified beside ZnO wurtzite in prepared ZnO. SEM images at ×1000 magnification shown in Fig. 5c, d reveal a significantly different morphology of TiO_2 and ZnO clusters. While conjunction of very fine nanoparticles of TiO_2 anatase forms spherical TiO_2 clusters, the nanoparticles of major ZnO wurtzite and minor Zn_2SiO_4 willemite form needle-like clusters and single needles. The surface energy of both materials was increased due to their small crystallite size and this feature led to agglomeration of crystallites.

TEM images and the evaluated TiO_2 anatase crystallite size distribution (Fig. 6a–c) correspond nicely to XRD results, proving the highest population of TiO_2 anatase crystallites of ~7 ± 2 nm size.

Acute biological toxicity

Acute biological toxicity tests on plants *L. minor* and *S. alba* showed toxic effects of both prepared nanostructured materials, TiO_2 as well as ZnO. However, ZnO demonstrated a significantly higher toxicity than TiO_2 (Fig. 7a, b).

Concerning the tests with *L. minor*, the inhibition of growth rate of *L. minor* was between 8.76 and 81.68% for TiO_2 and between 46.79 and 63.54% for ZnO. The inhibition of the weight of the final biomass of *L. minor* ranged from 31.90 to 91.48% for TiO_2 and from 21.73 to 86.63% for ZnO. Thus, the resulting EC_{50} toxicity values calculated from the inhibition growth rate of *L. minor* are following: 5.215 ± 0.138 mg/ml for TiO_2 and 1.839 ± 0.161 mg/ml for ZnO.

Concerning the tests with *S. alba*, the inhibition of *S. alba* root growth for TiO_2 was observed in the range of 12.01–60.48% and for ZnO in the range of 30.04–76.07%. The resulting IC toxicity values calculated from the inhibition of root growth are following: 172.853 ± 22.160 mg/ml for TiO_2 and 1.532 ± 0.930 mg/ml for ZnO. TiO_2 showed significantly lower toxic effect on seeds of *S. alba* compared to proven toxicity on *L. minor*.

The commercially available TiO_2 Degussa P25 did not show any toxic effects in both bioassays used, conversely to that the stimulation of *L. minor* frond growth was observed.

For comparison of the intensity of toxic effect, toxicological indexes EC_{50} and IC_{50} of nanoparticulated materials were compared with the positive controls of reference substances (3,5-dichlorophenol and potassium dichromate) and all results are summarized in Table 2.

Discussion of the obtained results and aspects related to toxicity of nanoparticulated ZnO, TiO_2 and commercially available TiO_2 Degussa P25 to *L. minor* and *S. alba*

Arruda et al. reported in their review (Arruda et al. 2015) that the mechanism of nanotoxicity is not still revealed. On the other hand, they reported that the nanotoxicity may be related to the chemical composition, chemical structure, particle-size and surface area of nanoparticles. The nanoparticles' toxicity may be explained by the following phenomena: (1) the chemical toxicity caused by the chemical composition, e.g. the release of (toxic) ions and (2) the stress or stimuli caused by the nanoparticles surface, size and/or shape. It was proved that the solubility of oxide nanoparticles markedly influences

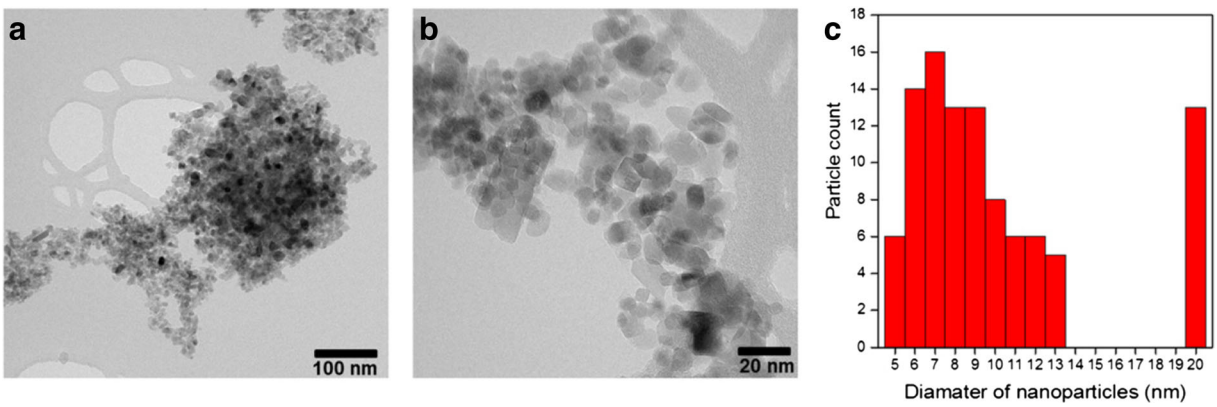

Fig. 6 TEM micrographs (**a**, **b**) with nanoparticle-size distribution (**c**) of prepared TiO_2

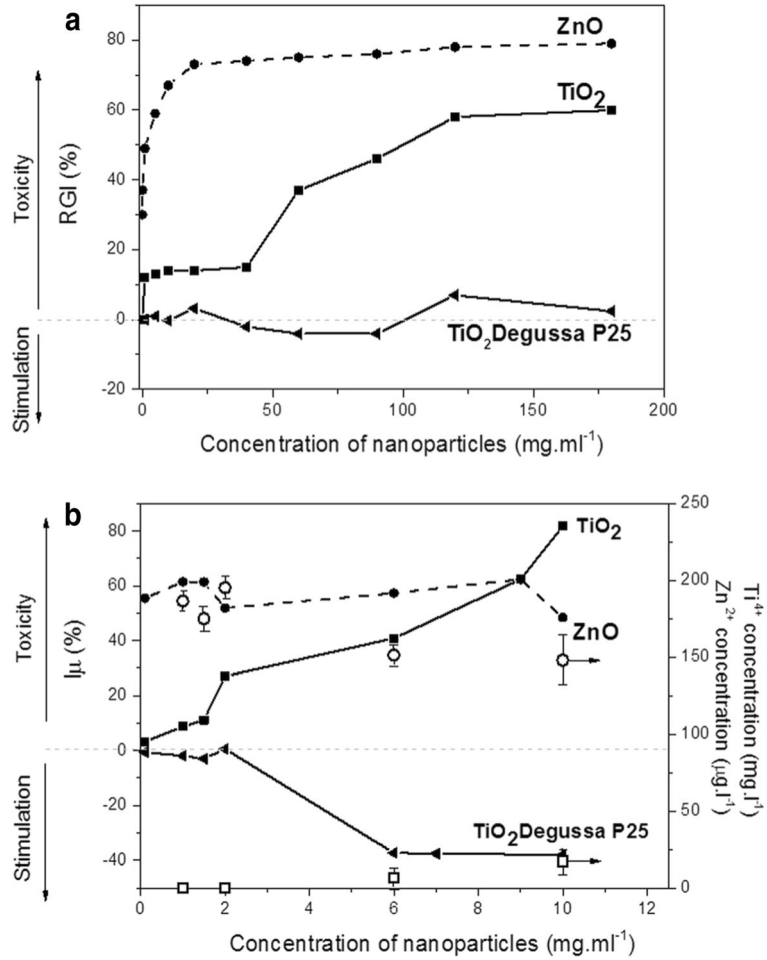

Fig. 7 Comparison of **a** *S. alba* root growth inhibition (RGI, %) and **b** growth inhibition of *L. minor* fronds (Iμ, %) in dependence on concentration of nanoparticles for all investigated nanoparticulated materials

the response of cell culture, and it was revealed that the nanoparticles-mediated toxicity cannot be exclusively attributed to the release of dissolved components of nanoparticles. They emphasized the fact that in many of studies both was not evaluated, the impacts of ions released from the nanoparticles as well as the impacts of nanoparticles on plants, thus, the gained results about nanoparticles toxicity may be confusing.

With respect to toxicity of nanoparticulated ZnO to *L. minor*, Chen et al. (Chen et al. 2016) investigated the toxicity of nanosized ZnO to *L. minor* via modulation of nanosized ZnO dissolution by either modification of the pH of the growth medium and/or surface coating of nanosized ZnO and evaluated the impacts on the growth and physiology of *L. minor*. Chen et al. revealed that nanosized ZnO was dissoluted quickly and completely in the medium at pH 4.5. Moreover, quantitatively similar toxic impacts were determined when *L. minor* was exhibited to nanosized ZnO as well as to the dissolved Zn equivalent of dissolved nanosized ZnO. Their

Table 2 Toxicological EC_{50} and IC_{50} indexes of investigated nanoparticulated materials and reference controls

	Material (mg/ml)			Reference substance (mg/ml)	
	ZnO	TiO_2	TiO_2 Degussa P25	3,5-Dichlorophenol	Potassium dichromate
EC_{50} (*Lemna minor*)	1.839 ± 0.161	5.215 ± 0.138	Stimulation	0.0037 ± 0.000026	–
IC_{50} (*Sinapis alba*)	1.532 ± 0.930	172.853 ± 22.160	No toxic effect	–	0.0421 ± 0.00245

conclusions that the toxicity of nanosized ZnO can be attributed to dissolved Zn^{2+} ions was further supported by the results that the phytotoxicity was missing in medium of higher pH values (>7). In those media, the dissolution of nanosized ZnO practically stopped. The decreased toxicity of coated nanosized ZnO, where the slower dissolution of Zn^{2+} ions took place, corresponded to the main role of dissolved Zn^{2+} ions in nanotoxicity of ZnO. Their results about the main role of released Zn^{2+} ions causing ZnO nanotoxicity support our obtained results. In our case, the synthesized ZnO is a mixture of larger nanoparticles of ~114 nm ZnO wurtzite and ~84 nm Zn_2SiO_4 willemite, having the surface area of 17 m^2/g. In spite of these larger crystallites of both crystalline phases, the toxicity of synthesized ZnO was significantly higher compared to "true" nanoparticulated TiO_2 anatase (~7 nm crystallite size, 240 m^2/g) especially to *S. alba*. Concerning the tests to *L. minor*, the toxicity of ZnO was even three times higher than of nanoparticulated TiO_2 (Table 2). Within the tests with *L. minor*, it was proved by AAS analysis that all nutrient aqueous solutions analysed after toxicity tests with ZnO contained the dissolved Zn^{2+} ions (Fig. 7b). The pH of the solutions moved between 6.5 and 7. Thus, our results support the fact that concerning the ZnO toxicity, the nanosize of crystallites and their surface area does not play the key role and the dissolution of Zn^{2+} ions to the nutrient medium contribute significantly to ZnO toxicity.

Li et al. (2013) examined the toxicity of nanoparticulated TiO_2-P25 (from Evonik industries AG, Essen, Germany), being the equivalent to investigated TiO_2 Degussa P25 in our study, to *L. minor*. In tests in order to exclude the nanoparticles aggregation and to achieve the *L. minor* exhibition to TiO_2 nanoparticles, they applied diluted growth medium. TiO_2 nanoparticles did not demonstrated any unfavourable impact on the growth rate of *L. minor*, even at a high exposure concentration of 5 mg/l and extended exposure time of 14 days. Despite of TiO_2 nanoparticles stuck to *L. minor* cell walls, no cellular uptake was observed. They concluded that albeit TiO_2 nanoparticles were not toxic to *L. minor*, there still exists the possibility of the transfer of TiO_2 nanoparticles in aquatic food chains and thus it can contribute to environmental negative impact of nanoparticles. In our study, without doing any additional dilution of growth medium and tests being done exactly according to ISO 20079 (2005) with *L. minor*, the stimulation of growth medium was observed in the presence of TiO_2 Degussa P25 nanoparticles at concentrations of nanoparticles above 6 mg/ml. Based on Li et al. observations (Li et al. 2013), it can be said in our case the aggregation of TiO_2 Degussa P25 nanoparticles definitively carried out in growth medium during the toxicity tests. Moreover, AAS analysis did not prove any dissolved Ti^{4+} ions in all nutrient solutions analysed after toxicity tests with TiO_2 Degussa P25. Thus, our results support and broaden the conclusions of Li et al. (2013) that TiO_2 Degussa P25 nanoparticles show no toxic effect to *L. minor*; even in aggregated form, they stimulate the growth of *L. minor* fronds.

Concerning the toxicity of synthesized nanoparticulated TiO_2 anatase, which toxicity was even about two orders lower to *S. alba* and three times lower to *L. minor* compared to ZnO (Table 2), it can be said that the exclusive effect of nanosize of TiO_2 crystallites or its high surface area on the toxicity to both plant species cannot be proved. In our case, the part of ~7-nm anatase crystallites was aggregated and the part stayed separately as nanoparticles, but these conditions do not affect the nanotoxicity of TiO_2 anatase crystallites in such a way to make it more toxic than ZnO to investigated plant species. On the other hand, with respect to TiO_2 toxicity, synthesized nanoparticulated TiO_2 anatase (~7 nm size) was toxic to both tested plant species contrary to TiO_2 Degussa P25 (anatase of ~25 nm size, rutile of ~54 nm size) which contrarily stimulated the growth of *L. minor* fronds and showed no toxic effect to *S. alba* seed. Thus, it can be concluded that in case of TiO_2 nanotoxicity, the complex effect of the rate of aggregation of nanosized TiO_2 crystallites, size, shape and surface properties will play the role in the stress and stimuli caused to both plant species. Moreover, from our results (Fig. 7a, b), it is evident that the toxicity of nanoparticulated TiO_2 depends significantly on the concentration of nanoparticles, being in contact with plant species. In case of TiO_2 anatase, its toxicity increased markedly from the nanoparticles concentration of 45 mg/ml for *S. alba* (Fig. 7a). Our observations about the effect of nanoparticles concentration on germination of *S. alba* are only in partial agreement with observations from Hatami et al. (2014). They reported contrarily on the stimulatory effect of nanosized TiO_2 anatase (of 10–15 nm crystallite size) on germination of *S. alba* in concentration range of 20–40 mg_{NPs}/ml. In tests with *L. minor*, the TiO_2 anatase toxicity was increasing gradually with increasing nanoparticles concentration in the range of 0.01–10 mg/ml (Fig. 7b).

Within tests with *L. minor*, AAS analysis of nutrient aqueous solutions analysed after toxicity tests, surprisingly, revealed that solutions with TiO_2 nanoparticle concentrations >6 mg/ml contained high concentrations of dissolved Ti^{4+} ions (Fig. 7b). Namely, Ti^{4+} ions concentrations were the following: 6.5 ± 0.2 mg/l for 6 $mg_{TiO2NPs}$/ml and 17.1 ± 0.8 mg/l for 10 $mg_{TiO2NPs}$/ml. These results indicate that even dissolution of Ti^{4+} ions from TiO_2 can take place at certain nanoparticle concentrations and this phenomenon may also contribute to TiO_2 toxicity. Whether the dissolution of Ti^{4+} ions from nanoparticulated TiO_2 will occur or not will be dependent on the type of chemical preparation and used titanium precursor.

Conclusions

Nanostructured TiO_2 and ZnO were prepared by unconventional processing using pressurized hot water in a flow regime, allowing the preparation of pure nanostructured materials at significantly lower temperature than during standard calcination. In case of TiO_2, the subsequent processing by pressurized hot water did not cause any significant changes within TiO_2 (micro)structure which was prepared by thermal hydrolysis. In case of ZnO, the processing by pressurized hot water affected crystallization of nanoparticles significantly. Detailed characterization of both prepared nanoparticulated materials revealed that TiO_2 anatase of ~7 nm crystallite size beside the mixture of major ZnO wurtzite (of ~114 nm crystallite size) and minor Zn_2SiO_4 willemite (of ~88 nm crystallite size) were formed under pressurized hot water. Tests of acute biological toxicity demonstrated a significant toxicity of ZnO. The eco-toxicity tests over ZnO showed the toxicity values EC_{50} = 1.839 ± 0.1605 mg/ml for *L. minor* and IC_{50} = 1.532 ± 0.930 mg/ml for *S. alba*. TiO_2 showing significantly lower crystallite size than ZnO exhibited markedly lower toxic effect on seeds of *S. alba* (IC_{50} = 172.853 ± 22.16 mg/ml) compared to proven, however, lower toxicity on *L. minor* fronds (EC_{50} = 5.215 ± 0.1375 mg/ml) than ZnO. The commercial TiO_2 Degussa P25 showed the growth stimulation effect to *L. minor* fronds and no toxic effect to *S. alba* root. It was shown the (micro)structural parameters such as the small crystallite size and the large surface area are not the acute biological toxicity-determining factors. The toxicity of TiO_2 nanoparticles to both plant species is affected by factors such as the rate of nanosized crystallites aggregation, their concentration, shape and surface properties. The dissolution of Ti^{4+} ions from TiO_2 nanoparticles can also occur at certain nanoparticle concentrations, possibly contributing to its toxicity. In case of ZnO nanotoxicity, the dissolution of Zn^{2+} ions is the main cause. Finally, it should be emphasized that the statement about TiO_2 non-toxicity should be taken with caution since it is significantly affected by used preparation method and/or used titanium precursors as seen in our case.

Compliance with ethical standards

Conflict of interest The authors declare that they have no conflict of interest.

Funding Financial support from the Grant Agency of the Czech Republic (project reg. No.14-23274S) is gratefully acknowledged. This work was also financially supported by EU structural funding Operational Programme Research and Development for Innovation (project No. CZ.1.05/2.1.00/19.0388). Authors' grateful thanks is also aimed to Dr. Pavel Buček from IET VŠB-Technical University of Ostrava for AAS analyses.

References

Adam V, Loyaux-Lawniczak S, Quaranta G (2015) Characterization of engineered TiO2 nanomaterials in a life cycle and risk assessments perspective. Environ Sci Pollut Res 22:11175–11192

Adams LK, Lyon DY, Alvarez PJJ (2006) Comparative eco-toxicity of nanoscale TiO_2, SiO_2, and ZnO water suspensions. Water Res 40:3527–3532

Andersen CP, King G, Plocher M et al (2016) Germination and early plant development of ten plant species exposed to titanium dioxide and cerium oxide nanoparticles. Environ Toxicol Chem 35:2223–2229

Arruda SCC, Silva ALD, Galazzi RM et al (2015) Nanoparticles applied to plant science: a review. Talanta 131:693–705

Arts JHE, Irfan MA, Keene AM et al (2015) Case studies putting the decision-making framework for the grouping and testing of nanomaterials (DF4nanoGrouping) into practice. Regul Toxicol Pharmacol 76:234–261

Barnes RJ, Molina R, Xu JB et al (2013) Comparison of TiO_2 and ZnO nanoparticles for photocatalytic degradation of methylene blue and the correlated inactivation of gram-positive and gram-negative bacteria. J Nanopart Res 15:1432–1443

Barrett EP, Joyner LG, Halenda PP (1951) The determination of pore volume and area distributions in porous substances. I. Computations from nitrogen isotherms. J Am Chem Soc 73: 373–380

Bellanger X, Billard P, Schneider R et al (2015) Stability and toxicity of ZnO quantum dots: interplay between nanoparticles and bacteria. J Hazard Mater 283:110–116

Bour A, Mouchet F, Silvestre J et al (2015) Environmentally relevant approaches to assess nanoparticles ecotoxicity: a review. J Hazard Mater 283:764–777

Chen XL, O'Halloran J, Jansen MAK (2016) The toxicity of zinc oxide nanoparticles to *Lemna minor* (L.) is predominantly caused by dissolved Zn. Aquat Toxicol 174:46–53

Clement L, Hurel C, Marmier N (2013) Toxicity of TiO_2 nanoparticles to cladocerans, algae, rotifers and plants–effects of size and crystalline structure. Chemosphere 90:1083–1090

Coronado JM, Fresno F, Hernández-Alonso MD et al (2013) Design of advanced photocatalytic materials for energy and environmental applications. Springer, London

Cox A, Venkatachalam P, Sahi S et al (2016) Silver and titanium dioxide nanoparticle toxicity in plants: a review of current research. Plant Physiol Biochem 107:147–163

de Boer JH, Lippens BC, Linsen BG et al (1966) Thet-curve of multimolecular N2-adsorption. J Colloid Interface Sci 21: 405–414

Farkas J, Peter H, Ciesielski TM et al (2015) Impact of TiO_2 nanoparticles on freshwater bacteria from three Swedish lakes. Sci Total Environ 535:85–93

Fu L, Hamzeh M, Dodard S et al (2015) Effects of TiO_2 nanoparticles on ROS production and growth inhibition using freshwater green algae pre-exposed to UV irradiation. Environ Toxicol Pharmacol 39:1074–1080

Gregg SJ, Sing KSW (1982) Adsorption, surface area and porosity. United States, New York

Hatami M, Ghorbanpour M, Salehiarjomand H (2014) Nano-anatase TiO_2 modulates the germination behavior and seedling vigority of some commercially important medicinal and aromatic plants. J Biol Eng 8:53–59

Hoffmann MR, Martin ST, Choi WY et al (1995) Environmental applications of semiconductor photocatalysis. Chem Rev 95: 69–96

Hofmann-Amtenbrink M, Grainger DW, Hofmann H (2015) Nanoparticles in medicine: current challenges facing inorganic nanoparticle toxicity assessments and standardizations. Nanomedicine-Nanotechnology Biology and Medicine 11: 1689–1694

Hougaard KS, Campagnolo L, Chavatte-Palmer P et al (2015) A perspective on the developmental toxicity of inhaled nanoparticles. Reprod Toxicol 56:118–140

Hsiao IL, Huang YJ (2011) Effects of various physicochemical characteristics on the toxicities of ZnO and TiO_2 nanoparticles toward human lung epithelial cells. Sci Total Environ 409:1219–1228

Jacob DL, Borchardt JD, Navaratnam L, Otte ML, Bezbaruah AN (2013) Uptake and translocation of Ti from nanoparticles in crops and wetland plants. Int J Phytoremediation 15(2):142–153

Judy JD, Bertsch PM (2014) Bioavailability, toxicity, and fate of manufactured nanomaterials in terrestrial ecosystems. Adv Agron 123:1–64

Kahru A, Dubourguier HC (2010) From ecotoxicology to nanoecotoxicology. Toxicology 269:105–119

Kumari M, Khan SS, Pakrashi S et al (2011) Cytogenetic and genotoxic effects of zinc oxide nanoparticles on root cells of *Allium cepa*. J Hazard Mater 190:613–621

Laborda F, Bolea E, Cepria G et al (2016) Detection, characterization and quantification of inorganic engineered nanomaterials: a review of techniques and methodological approaches for the analysis of complex samples. Anal Chim Acta 904:10–32

Lecloux A, Pirard JP (1979) The importance of standard isotherms in the analysis of adsorption isotherms for determining the porous texture of solids. J Colloid Interface Sci 70:265–281

Li L, Sillanpaa M, Tuominen M et al (2013) Behavior of titanium dioxide nanoparticles in *L. minor* growth test conditions. Ecotoxicol Environ Saf 88:89–94

Lin DH, Xing BS (2007) Phytotoxicity of nanoparticles: inhibition of seed germination and root growth. Environ Pollut 150: 243–250

Ma HB, Williams PL, Diamond SA (2013) Ecotoxicity of manufactured ZnO nanoparticles–a review. Environ Pollut 172:76–85

Mallevre F, Fernandes TF, Aspray TJ (2014) Silver, zinc oxide and titanium dioxide nanoparticle ecotoxicity to bioluminescent Pseudomonas putida in laboratory medium and artificial wastewater. Environ Pollut 195:218–225

Manke A, Wang LY, Rojanasakul Y (2013) Mechanisms of nanoparticle-induced oxidative stress and toxicity. Biomed Res Int. doi:10.1155/2013/942916

Manzo S, Rocco A, Carotenuto R et al (2011) Investigation of ZnO nanoparticles' ecotoxicological effects towards different soil organisms. Environ Sci Pollut Res 18:756–763

Matejova L, Koci K, Reli M et al (2013) On sol-gel derived Au-enriched TiO_2 and TiO_2-$OZrO_2$ Photocatalysts and their investigation in photocatalytic reduction of carbon dioxide. Appl Surf Sci 285:688–696

Matějová L, Kočí K, Troppová I et al (2017) TiO_2 and nitrogen doped TiO_2 prepared by different methods; on the (micro)structure and photocatalytic activity in CO_2 reduction and N_2O decomposition. J Nanosci Nanotechnol. doi:10.1166/jnn.2017.13936

Menard A, Drobne D, Jemec A (2011) Ecotoxicity of nanosized TiO_2. Review of in vivo data. Environmental Pollution 159: 677–684

Mukherjee A, Peralta-Videa JR, Bandyopadhyay S, et al (2014) Physiological effects of nanoparticulate ZnO in green peas (*Pisum sativum* L.) cultivated in soil. Metallomics 6:132–138

Priester JH, Ge Y, Mielke RE et al (2012) Soybean susceptibility to manufactured nanomaterials with evidence for food quality and soil fertility interruption. Proc Natl Acad Sci U S A 109: E2451–E2456

Quality Water (2005) Determination of the toxic effect of water constituents and waste water to duckweed (*Lemna minor*)–duckweed growth inhibition test (ISO CD 20079)

Rasmussen K, Gonzalez M, Kearns P et al (2016) Review of achievements of the OECD Working Party on Manufactured Nanomaterials' Testing and Assessment Programme. From exploratory testing to test guidelines. Regul Toxicol Pharmacol 74:147–160

Rico CM, Majumdar S, Duarte-Gardea M, et al (2011) Interaction of nanoparticles with edible plants and their possible implications in the food chain. J Agric Food Chem 59:3485–3498

RRUFF (2016) On-line database, http://rruff.info/Willemite/R100109 (Willemite R100109, accessed 26/5/2016).

Sadiq IM, Dalai S, Chandrasekaran N et al (2011) Ecotoxicity study of titania (TiO_2) NPs on two microalgae species: Scenedesmus sp and Chlorella sp. Ecotoxicol Environ Saf 74:1180–1187

Schiavo S, Oliviero M, Miglietta M et al (2016) Genotoxic and cytotoxic effects of ZnO nanoparticles for *Dunaliella tertiolecta* and comparison with SiO_2 and TiO_2 effects at population growth inhibition levels. Sci Total Environ 550: 619–627

Schneider P (1995) Adsorption isotherms of microporous-mesoporous solids revisited. Appl Catal A Gen 129:157–165

Sun TY, Gottschalk F, Hungerbuhler K et al (2014) Comprehensive probabilistic modelling of environmental emissions of engineered nanomaterials. Environ Pollut 185: 69–76

Tripathi DK, Shweta, Sing S et al (2017) An overview on manufactured nanoparticles in plants: uptake, translocation, accumulation and phytotoxicity. Plant Physiol Biochem 110: 2–12

Wang D, Lin Z, Wang T et al (2016) Where does the toxicity of metal oxide nanoparticles come from: the nanoparticles, the ions, or a combination of both? J Hazard Mater 308:328–334

Warheit DB, Boatman R, Brown SC (2015) Developmental toxicity studies with 6 forms of titanium dioxide test materials (3 pigment-different grade & 3 nanoscale) demonstrate an absence of effects in orally-exposed rats. Regul Toxicol Pharmacol 73:887–896

Xiong DW, Fang T, Yu LP et al (2011) Effects of nano-scale TiO_2, ZnO and their bulk counterparts on zebrafish: acute toxicity, oxidative stress and oxidative damage. Sci Total Environ 409:1444–1452

Yoon SJ, Kwak JI, Lee WM et al (2014) Zinc oxide nanoparticles delay soybean development: a standard soil microcosm study. Ecotoxicol Environ Saf 100:131–137